

# New Displacement-Sensing Techniques for Magnetic Bearings

Li Lichuan

Department of Electrical Engineering, Xi'an Jiaotong University, Xi'an, China  
email: lcli@mail.xjtu.edu.cn

**Abstract:** We report three new displacement-sensing techniques for magnetic bearings. An outstanding feature is that a carrier wave or demodulation is not needed, while performances comparable to that of existing techniques are obtained. The first is based on eddy-current energy loss, and has very simple sensor electronics. The second is capacitance type. It works by cyclic charge and discharge of a capacitor, and allows for direct fabrication on printed circuit board. The third is inductance type. It permits sensing across a 0.5-mm thickness wall of non-magnetic stainless-steel material, while the bandwidth is a few kHz.

**Keywords:** Displacement Sensors, Eddy-Current Testing, Capacitive Testing, Inductive Testing, Displacement Measurement, Switching Circuits

## Introduction

A magnetic bearing needs a number of displacement sensors. People who develop magnetic bearings also develop the displacement sensors. The reasons are two-fold. In some cases commercially available sensors satisfy all the technical requirement, but are too expensive. In other cases the commercially available sensors cannot be used, since the structure or size are not suitable.

Displacement sensing for magnetic bearings has been addressed in many papers. A variety of displacement sensors suitable for magnetic bearings are discussed and compared [1], with a conclusion that the eddy-current type is preferable. A capacitance-type displacement sensor with an arrangement suitable for magnetic bearings is presented [2]. Another capacitance-type displacement sensor is design and implemented [3], where the sensor electrode is fabricated on printed circuit board (PCB), and can be placed between the magnet poles so that sensors and bearings collocate. An inductive sensing system with synchronous detection is developed [4], where the displacement is sensed across a non-magnetic stainless steel wall. In order to achieve precise positioning of an AMB spindle, performance of a cylindrical capacitance-type displacement sensor is investigated [5]. Reflective optical sensors are successfully applied as displacement sensors [6], where the sensors are embedded in the stator to offer low mounting cost and sensor-bearing collocation. Satisfactory resolution and bandwidth are achieved by a low-cost inductance-type displacement sensor which demodulates the switching ripple [7]. A capacitance-type displacement sensor is designed such that the radial and axial displacements are both sensed by a single structure [8]. Cost-effective and high-performance displacement sensors, with sensor heads integrated in a mounting ring or sensing coils fabricated on PCB, are designed and tested [9]. A differential transformer displacement sensor is designed and successfully applied in magnetic bearings [10]. Performance of demodulation methods for inductance-type displacement sensors are investigated [11], showing that synchronous and non-synchronous demodulations yield similar results. Eddy-current displacement sensors are developed, with an integration of both the sensor heads and electronics [12]. To suspend a very

small rotor in a micro magnetic bearing, where the placement of a sensor is difficult, the capacitance between the rotor and stators are used to yield a displacement [13].

In this paper, we report three new displacement-sensing techniques. The first is based on eddy-current energy loss, the second is capacitance type, while the third is inductance type. Our techniques differ from others in many ways. An outstanding feature is that a carrier wave or demodulation is not needed, while performances comparable to that of existing techniques are obtainable.

### Displacement Sensing by Eddy-Current Energy Loss

Displacement sensing by eddy-current energy loss is easy to explain [14]. Shown in Fig. 1 is a circuit that explains the principle. Similar to the standard eddy-current displacement sensor, we use a sensing coil, which is represented by the inductance  $L$  and copper resistance  $R$ . The circuit is powered by a dc voltage source  $U$ . The oscillator gives a square-wave voltage output of a fixed frequency, 50% duty factor, and constant amplitude. The capacitor  $C_2$  prevents dc current from flowing through  $L$ , and is sufficiently large such that the voltage across it is almost constant. The capacitor  $C_1$  and resistor  $R_1$  form a low pass filter. Thus the current  $i$  can be viewed as ripple-free.

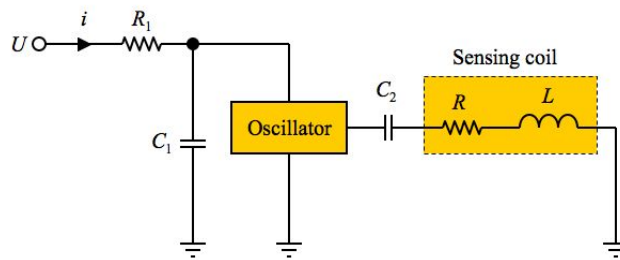


Fig. 1 A sensing coil driven by a square-wave voltage.

As a result, a square-wave voltage (of amplitude  $U/2$ ) is applied to the coil. This establishes a cyclic energy flow between the circuit and sensing coil. Because of energy losses in the coil, in each cycle the energy that returns from the coil to the circuit is less than that goes from the circuit to the coil. This cyclic energy loss forms a power loss, and the circuit must draw the same amount of power from the voltage source  $U$ . Thus  $i$  is a function of the energy losses. Moreover, as a conductive sensor target approaches the coil, the energy losses at the coil side (within both coil and target material) increase, and  $i$  increases.

Mathematical analysis of the dependence of  $i$  on target displacement is much more difficult than experiment study, so we use the latter method to investigate the performances. In one of our tests,  $i$  increases from 2.4 to 3.1 mA as a target is displaced toward the coil by 1 mm [14], showing a nontrivial sensitivity and a significant relative change in  $i$ . In this test, the coil has a diameter of 5.5 mm and has 50 turns, the target material is aluminum,  $U$  is 3.3 V, and the square-wave frequency is 1.8432 MHz. More details are found in [14]. Results with different parameters and configurations, and using different target materials, are found in [15].

We have developed displacement sensors on this principle, as shown in Fig. 2. The sensor electronics of Fig. 1, except  $R_1$ , is placed inside the sensor body. The sensor output versus displacement is nonlinear [14]. Instead of linearization, we use two such sensors for a single motion axis (in a differential configuration, see Fig. 2), which gives satisfactory linearity. When

$R_1$  is small such that voltage drops on it is much smaller than  $U$ , the bandwidth is approximated by  $1/2\pi R_1 C_1$ . Test shows that at a 10-kHz bandwidth the peak-to-peak noise is no more than 1  $\mu\text{m}$ . The potentiometer  $W$  is for removal of offset between the two sensors.

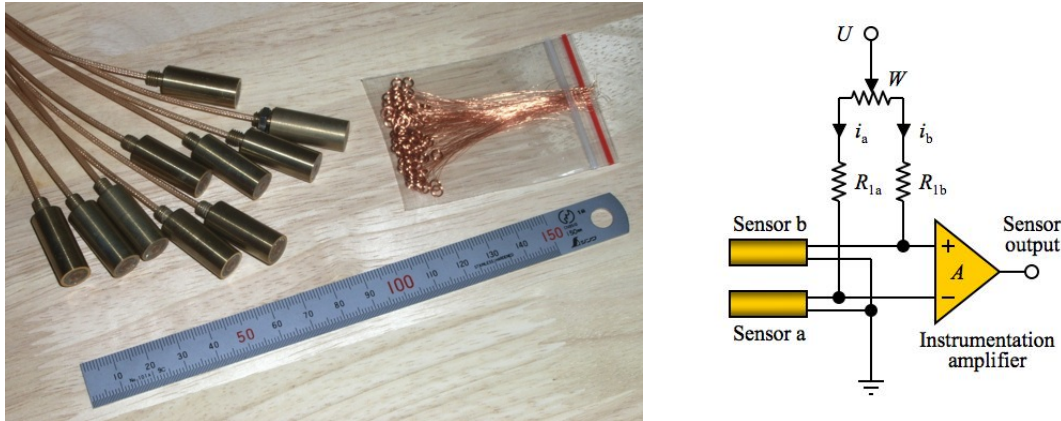


Fig. 2 Sensors with electronics enclosed (left) and differential configuration (right).

### Capacitive Displacement Sensing by Cyclic Charge and Discharge

The principle of this type is also very simple and easy to explain. Shown in Fig. 3 is a circuit that explains the principle, where  $K_1$  and  $K_2$  are ideal switches and operate in complement, at a fixed switching frequency  $f$ , and a fixed duty factor of 50%. The capacitor  $C$  represents the capacitance formed by an air gap being measured. The resistor  $R$  removes the singularity at the instant  $K_1$  and  $K_2$  change states. The rest of the circuit is the same as that of Fig. 1.

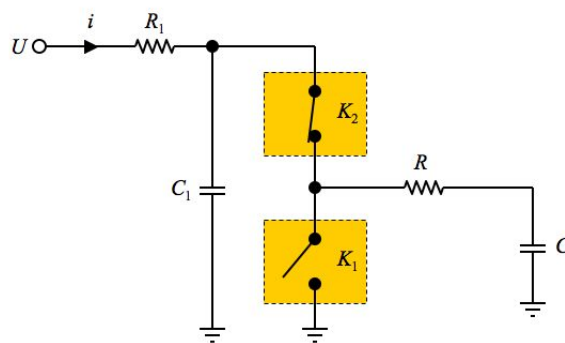


Fig. 3 Circuit for cyclic charge and discharge of the capacitor  $C$ .

Consider a single switching cycle. Let  $RC \ll T/2$ , where  $T = 1/f$  is the period of a cycle. Then, in the first half of a switching cycle,  $K_1$  is open and  $K_2$  closed, and  $C$  is charged to a voltage close to  $U$  (since  $RC \ll T/2$ ). In the second half,  $K_1$  is closed and  $K_2$  open, and  $C$  is discharged. Thus the circuit draws an electrical charge of  $CU$  in a switching cycle, and the current  $i$  is given by  $i = fCU$ .

Unlike the case of the previous section, where  $i$  typically changes by 1 mA, here the change in  $i$  caused by a change in  $C$  is much smaller. Take a reasonable  $f$  of 4 MHz,  $U$  of 5 V, and a typical change in  $C$  of 0.1 pF, then the change in  $i$  is only 2  $\mu\text{A}$ . So we should be careful when design

actual circuit. The oscillator in Fig. 1 cannot be used, since the oscillator itself draws a substantial current from  $U$  that is much larger than  $2 \mu\text{A}$ , giving a very small relative change in  $i$ . So the switches in Fig. 3 should be explicitly implemented using small-signal MOSFETs as shown in Fig. 4. As the MOSFETs are being switched, a current is also drawn from  $U$ , but is much smaller than that of a self-contained oscillator. This current is also proportional to the switching frequency, and can be modeled by a fictitious capacitor  $C_0$  in parallel with  $C$ . Using commercially available components, a  $C_0$  of as small as a couple of pF is easily achieved.

In Fig. 4, when  $R_1$  is small such that voltage drops on it is much smaller than  $U$ , the circuit on the left is equivalently described by that on the right. If the voltage drop on  $R_1$  is taken as sensor output, then the sensor has a first-order dynamics and a bandwidth of  $1/2\pi R_1 C_1$ .

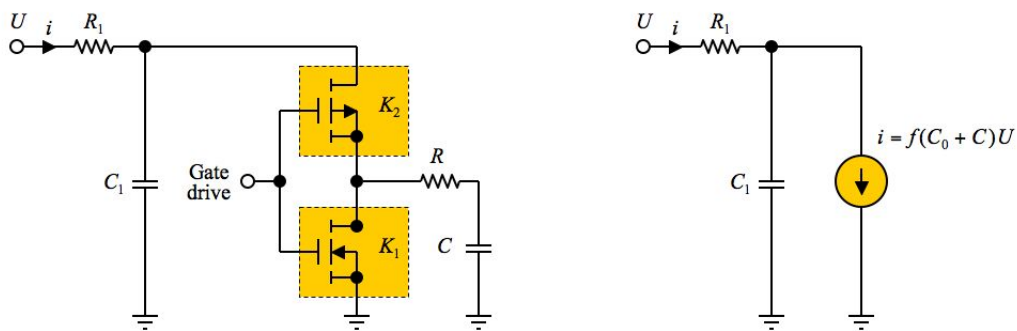


Fig. 4 Circuit with ideal switches replaced by small-signal MOSFETs (left) and the equivalent (right).

We have developed radial displacement sensors according to this principle. Four channels are arranged on a single piece of PCB, as shown in Fig. 5. Standard CMOS inverters are used as the switches. A pair of opposing channels form a differential configuration and measure a single motion axis, as sketched in Fig. 6. For each channel, the sensing surface is formed by the cross-section of a double-layer copper plate (see Fig. 6). The copper plate has a 0.035-mm thickness and 7-mm width, giving a sensing area of  $2 \times 7 \times 0.035 = 0.49 \text{ mm}^2$ . But, because of flux stray, the actual sensing area is much larger. The nominal air gap between the sensing surface and the conductive rotor is  $d_0 = 0.2 \text{ mm}$ . The voltage drops caused by  $i_a$  and  $i_b$  are differentially amplified by the amplifier  $A$ . Offset between the two channels is removed by the potentiometer  $W$ . By  $U = 5 \text{ V}$  and  $f = 4 \text{ MHz}$ , a 0.3- $\mu\text{m}$  peak-to-peak noise along with a 8-kHz bandwidth is obtained.

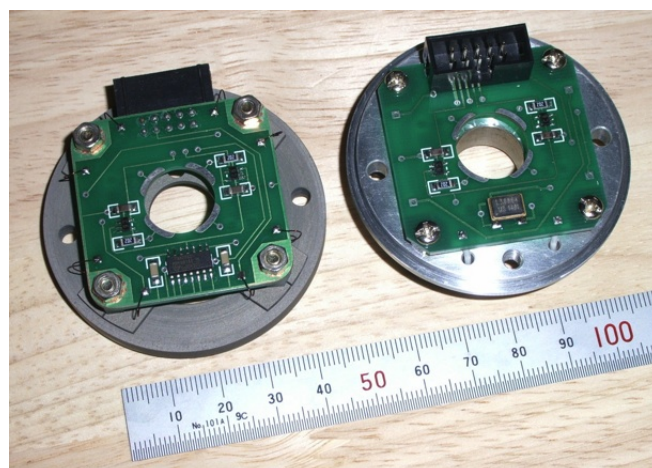


Fig. 5 Radial displacement sensors on PCB (coils of radial bearings are routed out from the PCB).

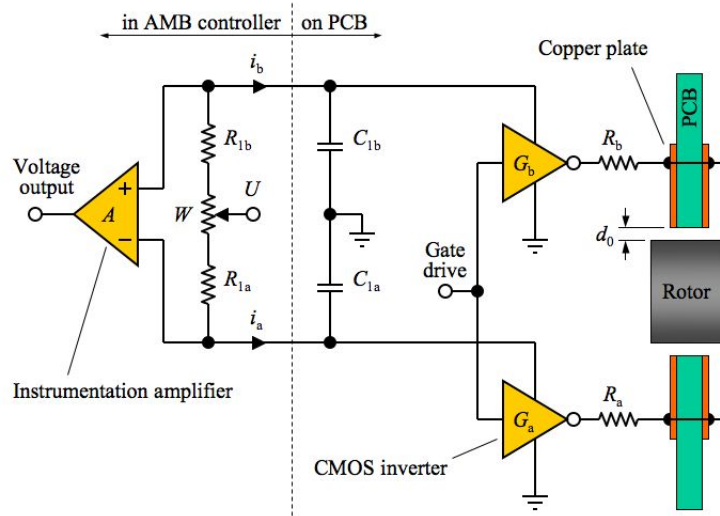


Fig. 6 Differential configuration of two channels for a single motion axis.

### Inductive Displacement Sensing by Direct Sampling

To explain our method, consider a single motion axis. Similar to existing methods, we use a pair of inductors,  $L_a$  and  $L_b$ , to form a differential configuration. Let  $L_a$  and  $L_b$  be represented by  $L_a = L - \Delta L$  and  $L_b = L + \Delta L$ , where  $L$  is the nominal inductance and  $\Delta L$  is the change of  $L$  caused by target motion.

The arrangement of the direct sampling is shown in Fig. 7. The one-shot multivibrator is repeatedly triggered by an AMB controller at its sampling frequency, and gives a square-wave voltage output. The capacitor  $C$  prevents dc current from flowing through the inductors, and has a sufficiently large capacitance such that the voltage across it is almost constant. So, in steady state, the voltage waveforms are as shown. Immediately prior to the issue of a trigger, the midpoint voltage  $u_m$  is sampled and converted to a digital value, at which moment the transient in  $u_m$  has almost gone (transient not shown in the waveforms). Then, immediately, a trigger is issued.

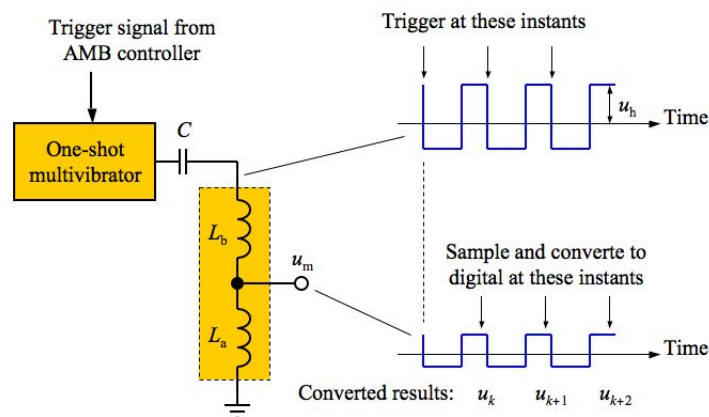


Fig. 7 Inductive displacement sensing by direct sampling.

Assume that the time constant  $L/R$  is much larger than the sampling interval, where  $R$  is the copper resistance of each inductor (not shown in Fig. 7), so voltage drops on  $R$  is negligible. Since  $L_a$  and  $L_b$  always see the same current change rate, and at a sampling instant the total voltage applied on  $L_a + L_b$  is  $u_h$  (see Fig. 7), we have  $u_k = (1/2 - \Delta L_k/2L)u_h$ , where  $\Delta L_k$  is the instant value of  $\Delta L$  when the sampling takes place.

It is clear that our design differs from existing ones only in signal processing, the sensor head (inductor cores and coils) being the same. By direct sampling, the carrier frequency is low, and sensing across a non-magnetic metal wall is possible [4]. We have developed radial sensors for our magnetic bearings as shown in Fig. 8, where  $L_a$  and  $L_b$  measure the horizontal axis, while  $L_c$  and  $L_d$  measure the vertical axis. The midpoint voltages  $u_{ab}$  and  $u_{cd}$  are sampled simultaneously. The sensor cores are mounted on the outside of a non-magnetic stainless-steel tube (so are magnetic bearing stator cores). The rotor is inside the tube. The wall thickness at the sensor position is 0.5 mm.

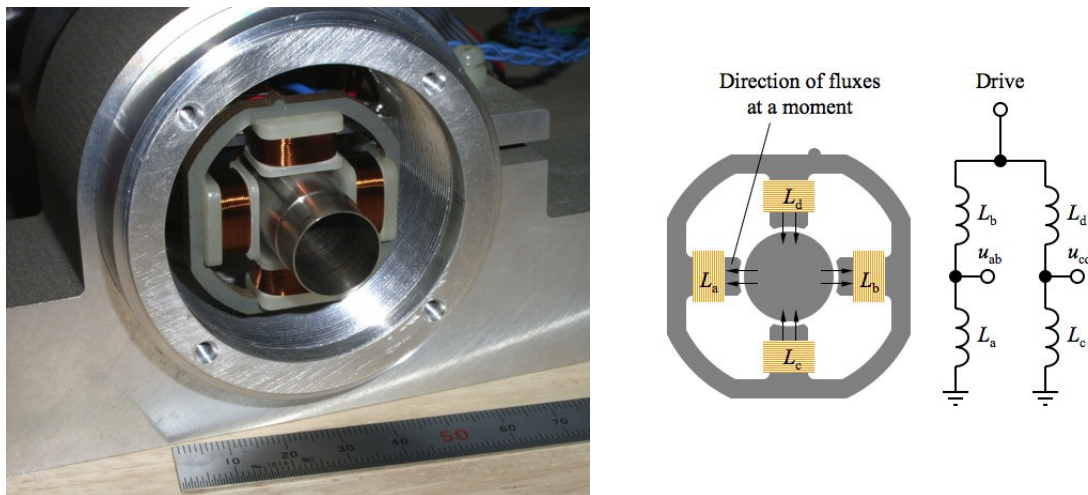


Fig. 8 Inductive displacement sensor that senses across a non-magnetic stainless-steel wall.

By comparing the magnetic bearing models identified when the rotor is suspended using the sensors of Fig. 8 and Fig. 5 respectively, we have a rough estimation of 3-kHz bandwidth of the present one. In the test the sampling frequency is 10 kHz. The midpoint voltages are sampled without any amplification. As the rotor is suspended, peak-to-peak positioning noise observed from the sampled data is  $2 \mu\text{m}$ . The stator is laminated, and the rotor is not. Up to a rotational speed of 140,000 rpm, the sensor gives correct displacement signals.

## Conclusions

We have presented the displacement-sensing techniques. We conclude the paper by making the following comments.

(1) The techniques have a common feature: simplicity. With regard to overall performance, the sensors presented may not be the best, but in our experience they have performances that are just enough for most magnetic bearings. The reason is obvious: they are developed solely for magnetic bearings.

(2) The eddy-current type has a high sensitivity (the raw sensitivity), and subsequent signal processing is easy. In our experience, a weakness is that the tiny and delicate coils are not easy

to handle and fix. Besides, the operating temperature is limited because the electronics is placed together with the coil. It is possible to place the electronics away from the coil, with some loss of sensitivity caused by the additional inductance of the connecting cable.

(3) The capacitance type is the most simple to fabricate, especially in mass production. But application of capacitive sensors require a clean environment, which is the main weakness of this type. Since the electronics is placed on the PCB, operating temperature is also limited.

(4) The inductance type is not too difficult to fabricate and easy to use. The geometry of the sensor core can be precisely controlled, and offset adjustment is not required. High operating temperature is possible. A weakness is the susceptibility to external changing magnetic field, since by direct sampling the sensor essentially works in baseband. Another weakness is that antialiasing filtering is impossible.

## References

- [1] J. Boehm, R. Gerber, and N.R.C. Kiley: Sensors for Magnetic Bearings, *IEEE Trans. Magnetics*, Vol. 29, No. 6, 1993, pp. 2962-2964.
- [2] A.O. Salazar, W. Dunford, R. Stephan, and E. Watanabe: A Magnetic Bearing System Using Capacitive Sensors for Position Measurement, *IEEE Trans. Magnetics*, Vol. 26, No. 5, 1990, pp. 2541-2543.
- [3] D. Shin and J. Kim: Design and Implementation of PCB-type Capacitance Displacement Sensor Collocated with Magnetic Bearings, *Sensors and Actuators A*, Vol. 71, 1998, pp. 223-229.
- [4] S. Moriyama, K. Watanabe, and T. Haga: Inductive Sensing System for Active Magnetic Suspension Control, *Proc. 6th Int. Symp. Magnetic Bearings*, 1998, pp. 529-537.
- [5] S. Jeon, H.J. Ahn, and D.C. Han: New Design of Cylindrical Capacitive Sensor for On-line Precision Control of AMB Spindle, *Proc. 7th Int. Symp. Magnetic Bearings*, 2000, pp. 495-500.
- [6] C. Klesen and R. Mordmann: Design of a Low Cost Active Magnet Bearing, *Proc. 7th Int. Symp. Magnetic Bearings*, 2000, pp. 455-460.
- [7] M.D. Noh, M.K. Jeong, B.C. Park, J.K. Park, and S.K. Ro: Development of a Low Cost Inductive Sensor Using Switching Noise Demodulation, *Proc. 8th Int. Symp. Magnetic Bearings*, 2002, pp. 311-314.
- [8] H.J. Ahn, I.H. Kim, and D.C. Han: A Novel Cylindrical Capacitive Sensor (CCS) for Both Radial and Axial Motion Measurement, *Proc. 9th Int. Symp. Magnetic Bearings*, 2004, pp. 118-123.
- [9] R. Larsonneur and P. Buehler: New Radial Sensors for Active Magnetic Bearings, *Proc. 9th Int. Symp. Magnetic Bearings*, 2004, pp. 86-90.
- [10] C. Jin, L. Xu, and J. Zhou: Application of Differential Transformer Displacement Sensors in Active Magnetic Bearings, *Proc. 1st China Symp. Magnetic Bearings*, 2005, pp. 455-460, in Chinese.
- [11] J. Zhao, Y. Zhou, Z. Shi, M. Zha, and L. Zhao: The Study of Two Inductance Displacement Sensor for AMB System, *Proc. 1st China Symp. Magnetic Bearings*, 2005, pp. 89-92, in Chinese.
- [12] C. Wang, Y. Hu, and X. Wang: The Integrated Magnetism Aerosol Rotor Displacement Synchronous Detection System Research, *Proc. 2nd China Symp. Magnetic Bearings*, 2007, pp. 89-91, in Chinese.
- [13] J. Kuroki, T. Shinshi, L. Li, and A. Shimokohbe: A Micro-Magnetic Bearing Using Capacitive Axial Displacement Sensing, *Precision Engineering*, Vol. 30, No. 1, 2006, pp. 54-62.
- [14] L. Li: Eddy-Current Displacement Sensing Using Switching Drive Where Baseband Sensor Output Is Readily Available, *IEEE Trans. Instrum. Meas.*, Vol. 57, No. 11, 2008, pp. 2548-2553.
- [15] J. Zhong and L. Li: Switch-Driving Eddy-Current Displacement Sensing Based on Power Loss, *Proc. 12th Int. Symp. Magnetic Bearings*, 2010, pp. (not yet known).